Seasonal Prediction over North America with a Regional Model Nested in a Global Model

M. J. FENNESSY AND J. SHUKLA

Center for Ocean–Land–Atmosphere Studies, Calverton, Maryland

(Manuscript received 14 January 1999, in final form 27 September 1999)

ABSTRACT

Ensembles of winter and summer seasonal hindcasts have been carried out with an 80-km resolution version of the National Centers for Environmental Prediction, Environmental Modeling Center Eta model over the North American region. The lateral boundary conditions for the Eta model are prescribed from Center for Ocean–Land–Atmosphere R40 atmospheric general circulation model integrations, which used observed atmospheric initial conditions and observed global sea surface temperature (SST).

An examination of 15 seasonal winter hindcasts and 15 seasonal summer hindcasts shows that the nested model reduces the systematic errors in seasonal precipitation compared to the global model alone. The physical parameterizations, enhanced resolution, and better representation of orography in the Eta model produces better simulations of precipitation, and in some cases, its interannual variability. In particular, the precipitation difference between the 1988 drought and 1993 flood over the United States was much better simulated by the nested model. The predictions of circulation features were generally as good or better than those from the global model alone.

Estimates of external (SST forced ''signal'') and internal (dynamics generated ''noise'') variability were made for both the global model and the nested model predictions. Contrary to the expectation that a higher-resolution model would have higher internal-dynamics-generated variability, the signal, noise, and signal-to-noise ratios of the near-surface temperature and precipitation fields were generally quite similar between the nested model and the global model predictions. In the winter season the nested model had larger signal-to-noise ratios in both temperature and precipitation than did the global model alone.

1. Introduction

Research during the past 20 yr has established that seasonal climate anomalies over continental regions are forced in part by slowly varying boundary conditions of sea surface temperature (SST) and land surface conditions. It is also well established that SST anomalies, particularly in the tropical oceans, can be predicted by coupled ocean–atmosphere models. It is therefore reasonable to expect that accurate predictions of boundary conditions would allow prediction of regional climate anomalies for lead times beyond the limit of deterministic predictability (Shukla 1998). However, the current atmospheric general circulations models (AGCMs) are unable to predict the regional precipitation anomalies over the continents even with prescribed observed global SST anomalies. Is this inability to predict regional precipitation a fundamental constraint of the predictability of the regional climate or is it due to the parameterizations and spatial resolution of the current AGCMs? The current AGCMs do not have sufficient horizontal resolution to resolve regional orographically forced precipitation features and a systematic study with a very high-resolution global AGCM to address this question would require more computer time than is currently available.

An alternate approach to address this question that requires less computing time is to use a low-resolution coupled ocean–land–atmosphere model to predict the anomalous surface boundary conditions of SST, soil wetness, and snow depth, which are the most important determinants of predictable seasonal to interannual climate variations. The predicted boundary conditions are then applied to a medium resolution global atmospheric model that is integrated for a season to produce the global circulation and planetary scale waves that occur in response to the anomalous boundary conditions. A limited-area high-resolution atmospheric model is then nested in the global atmospheric model by applying the global circulation predicted by the medium resolution model as a lateral boundary condition to the high-resolution regional model. Given a sufficiently large domain for the nested model, this matching at the boundaries specifies only the continental-scale heat and moisture flux divergences and allows the actual distribution of temperature and precipitation within the domain to

Corresponding author address: Mr. M. Fennessy, COLA, 4041 Powder Mill Rd., Suite 302, Calverton, MD 20705.
E-mail: fen@cola.iges.org

be significantly different from that of the global model. The regional climatic details that are indistinct or even erroneous in the medium resolution model could be more skillfully predicted by the high-resolution model. This procedure allows us to address the following question: can the predictable component of the large-scale atmospheric circulation be used in conjunction with high-resolution regional dynamical models to predict regional climate in North America at seasonal and longer lead times? Results of Giorgi and Bates (1989) and Giorgi (1990) for the western United States, Ji (1996) and Ji and Vernekar (1997) for the Indian monsoon region, and of Tanajura (1996) for the South American region, among others, have already provided strong evidence for scientific justification of this procedure. This paper presents hindcasts of North American regional climate using the Eta model nested in the Center for Ocean–Land-Atmosphere (COLA) AGCM.

Because the lead time of interest is longer than the inherent limit of deterministic predictability of instantaneous atmospheric flows, an element of uncertainty is present at each step of the procedure outlined above. In order to make the predictions more robust and to quantify the uncertainty, it is necessary to make multiple realizations with each model. The multiple realizations are produced by perturbing the initial conditions used in each model and repeating the model integration with each of the perturbed initial states.

An 80-km version of the National Centers for Environmental Prediction (NCEP) Environmental Modeling Center (EMC) Eta model (Black 1994) centered over North America is nested in the COLA R40 global AGCM for seasonal integrations. The Eta model was chosen following the successful results of Ji and Vernekar (1997) in simulating seasonal mean features and interannual variability of the Indian summer monsoon rainfall, and Tanajura (1996) in simulating the South American climate, both using the Eta model. In this hindcast experiment, both models utilize the same time-varying observed weekly SST (Reynolds and Smith 1994). Otherwise, the AGCM receives no additional input after initialization and the nested Eta regional model receives only the lateral boundary conditions from the AGCM at 12-h intervals. The frequency of the lateral boundary updating was determined by the availability of AGCM output from existing integrations. Ensembles of three nested integrations for each of five different years are performed and compared with observations and with integrations of the GCM alone.

The model formulations and experimental design are described in section 2. The seasonal mean climate hindcasts are presented in section 3. Aspects of the simulation of the observed interannual variability, including systematic and root-mean-square (rms) errors, are discussed in section 4. Signal-to-noise calculations are presented in section 5. Conclusions and further work required are discussed in section 6.

2. Models and experimental design

a. COLA AGCM

The COLA GCM is based on a modified version of the NCEP global spectral model used for medium-range weather forecasting [see Sela (1980) for original NCEP formulation; see Kinter et al. (1988; 1997) and Dewitt (1996) for the modified version]. The land surface parameterization was changed to the Simple Biosphere Model biophysical formulation after Sellers et al. (1986) by Sato et al. (1989) and later simplified by Xue et al. (1991). The model uses relaxed Arakawa–Schubert convection (Moorthi and Suarez 1992; after Arakawa and Schubert 1974), and Tiedtke (1984) shallow convection after Hogan and Rosemond (1991), and is described by Dewitt (1996).

The COLA GCM is a global spectral model with rhomboidal truncation at zonal wavenumber 40 (R40). The model physics calculations are done on a 1.8° lat $\times$ 2.8° long Gaussian grid. The vertical structure of the model is represented by 18 unevenly spaced levels using σ as the vertical coordinate (Phillips 1957). The spacing of the levels is such that greater resolution is obtained near the earth's surface and at the tropopause. In addition to the parameterizations mentioned above, the COLA GCM includes parameterizations of solar radiative heating (Lacis and Hansen 1974), terrestrial radiative heating (Harshvardhan et al. 1987), large-scale condensation, interactive cloud–radiation (Hou 1990; after Slingo 1987), gravity wave drag (Vernekar et al. 1992; after Alpert et al. 1988) and a turbulence closure scheme for subgrid-scale exchanges of heat, momentum, and moisture (Miyakoda and Sirutis 1977; Mellor and Yamada 1982).

In the COLA GCM, each land grid box (approximately 1.8° lat $\times$ 2.8° long) is assigned one of twelve sets of vegetation and soil characteristics, based on the dominant vegetation observed in the grid box (Dorman and Sellers 1989; Fennessy and Xue 1997). Included in these characteristics are the depth and porosity of each of three soil layers: the surface layer, the root zone, and the drainage layer. The total depth of the three layers ranges from 49 cm for bare soil (desert) to 350 cm for trees. The total water holding capacity ranges from 21 cm for bare soil to 147 cm for trees. The soil wetness is initialized from proxy seasonally varying soil wetness derived from data produced by the European Centre for Medium-Range Weather Forecasts (ECMWF) analysis–forecast system (Fennessy and Shukla 1996). The model uses mean orography calculated from the U.S. Navy 10-min elevation data.

b. NCEP EMC Eta regional model

The regional model used in this study is a slightly modified version of the NCEP EMC Eta model that became operational in March 1997. For the sake of computational efficiency the horizontal resolution was re-

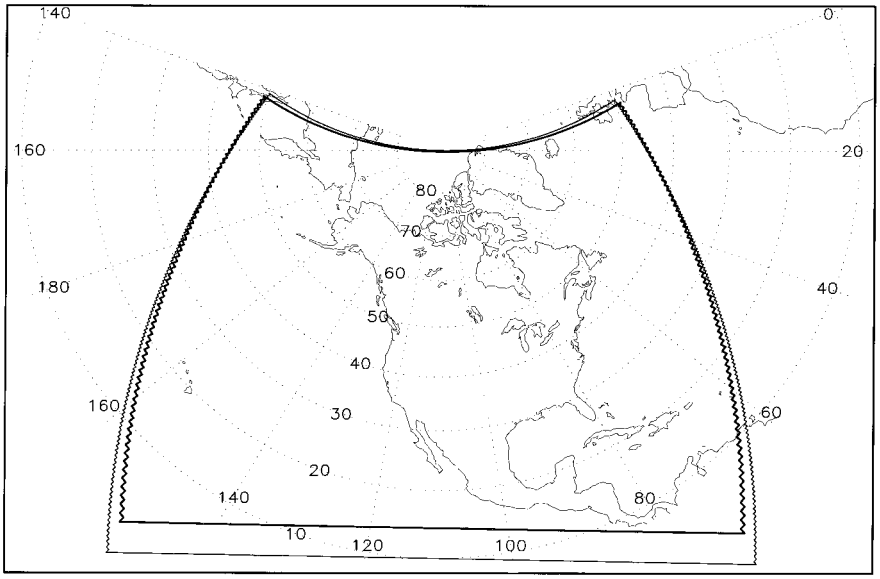

FIG. 1. Integration domain of (a) the 80-km Eta used in this study (dark) and (b) the Mar 1997 operational 48-km Eta (light).

duced from 48 to 80 km (as used operationally until October 1995). Aside from changing the horizontal resolution, the model is almost identical to the operational version, which is routinely run for 48 h, except for procedural changes, which were necessary to make longer climate integrations and to nest the model in the COLA R40 AGCM. The 80-km regional model integration domain used here (92 × 141 grid, Fig. 1, heavy line) is nearly identical to the ''early'' Eta 48-km domain used operationally in March 1997 (160 × 261 grid, Fig. 1., light line).

The Eta model is a state-of-the-art mesoscale weather forecast model with an accurate treatment of complex topography using the eta vertical coordinate and steplike mountains (Mesinger 1984), which eliminates errors in the pressure gradient force over steeply sloped terrain present in sigma coordinates (Mesinger and Black 1992). The recent version used here follows that described by Mesinger et al (1988), Black (1994), Rogers et al. (1995; 1996), and Mesinger (1996). The model employs a semistaggered Arakawa E-grid in which wind points are adjacent to mass points (Arakawa and Lamb 1977), configured in rotated spherical coordinates. There are 38 Eta vertical levels and the model top is at 50 mb. Split-explicit time differencing is used with a 120-s adjustment time step. Space differencing is done with a conserving Arakawa-type scheme (Janic 1984). The eta steplike mountains are derived from the silhouette-mean orography of Mesinger (1995). The orography used in the COLA AGCM, the nested Eta model, and their difference is shown in Figs. 2a–c, respectively. Large differences of up to 500 m or more occur in the vicinity of the Sierra Nevada and the Rocky, and Appalachian Mountains. In particular, the latter are present in the Eta orography (Fig. 2b) and all but absent in the COLA AGCM orography (Fig. 2a).

The model physics has been described by Janjic (1990, 1994) and includes a modified Betts–Miller scheme for deep and shallow convection (Betts and Miller 1986; Janjic 1994), and predicted cloud water/ice (Zhao et al. 1997). The GFDL scheme is used for radiation (Fels and Schwarztkopf 1975; Lacis and Hansen 1974). Free atmospheric turbulent exchange above the lowest model layer is via Mellor–Yamada (1982) level 2.5, and the surface layer similarity functions are derived from Mellor–Yamada level 2.0 (Lobocki 1993). A viscous sublayer is used over water surfaces (Janjic 1994). The land surface is a version of the Oregon State University scheme modified by Chen et al. (1997).

c. Experimental design

The COLA AGCM integrations were done first and data were saved every 12 h. For each of the COLA AGCM integrations a nested integration with the Eta model was done, starting from the same initial date and initial data as the AGCM and using as lateral boundary conditions the 12-h AGCM data linearly interpolated in time. This one-way nesting technique is similar to that used by Ji and Vernekar (1997) and uses a two gridpoint overlap as used operationally at NCEP.

The 15 summer integrations were initialized in late May and span all of June–September (JJAS). The 15 winter integrations were initialized in mid December and span all of January–March (JFM). All the integrations were initialized from analyses of the observations, either from the National Meteorological Center (now known as NCEP) operational analyses, the NCEP re-

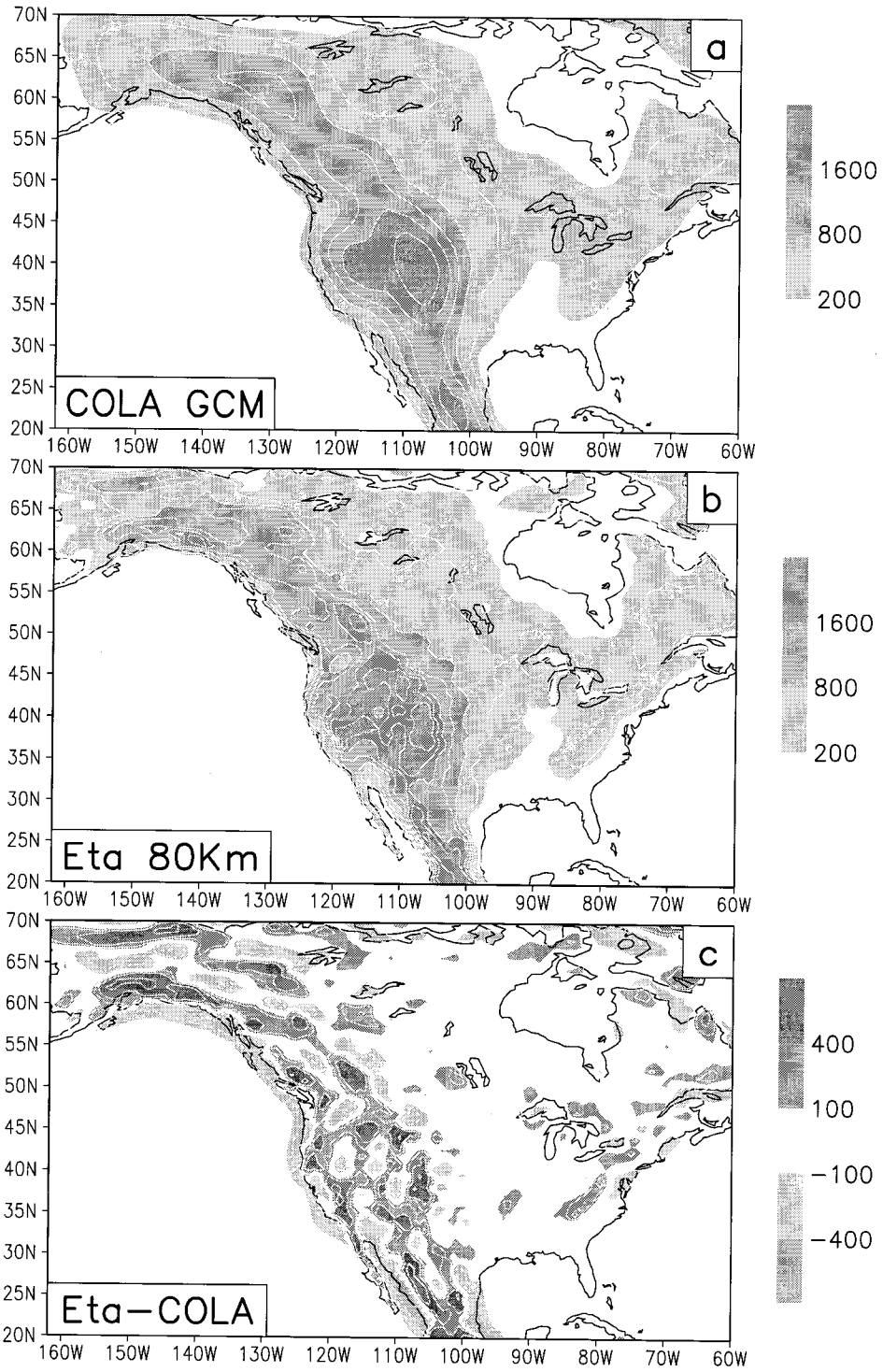

FIG. 2. Orography used for (a) COLA AGCM, (b) nested Eta, and (c) difference. Contours are 100, 200, 400, 800, 1200, 1600, 2000, and 2400 m.

analyses, or the COLA reanalyses. The integration initial dates and initialization data sources are given in Table 1. The years were chosen from a set of preexisting COLA AGCM integrations. This choice was biased toward ENSO years and years with significant North American climate anomalies.

Observed time-varying weekly SST (Reynolds and Smith 1994) was linearly interpolated in time and used

TABLE 1. Integration initial dates and initialization data sources.

Summer integrations		Winter integrations	
0000 UTC 29 May 1986	NCEP reanalysis	0000 UTC 13 Dec 1982	COLA reanalysis
0000 UTC 30 May 1986	NCEP reanalysis	1200 UTC 13 Dec 1982	COLA reanalysis
0000 UTC 31 May 1986	NCEP reanalysis	0000 UTC 14 Dec 1982	COLA reanalysis
0000 UTC 28 May 1987	NMC analysis	0000 UTC 13 Dec 1984	NCEP reanalysis
1200 UTC 28 May 1987	NMC analysis	1200 UTC 13 Dec 1984	NCEP reanalysis
0000 UTC 29 May 1987	NMC analysis	0000 UTC 14 Dec 1984	NCEP reanalysis
0000 UTC 28 May 1988	NMC analysis	0000 UTC 13 Dec 1986	NMC analysis
1200 UTC 28 May 1988	NMC analysis	1200 UTC 13 Dec 1986	NMC analysis
1200 UTC 30 May 1988	NMC analysis	1200 UTC 14 Dec 1986	NMC analysis
0000 UTC 28 May 1993	NMC analysis	0000 UTC 13 Dec 1988	NCEP reanalysis
1200 UTC 28 May 1993	NMC analysis	1200 UTC 13 Dec 1988	NCEP reanalysis
0000 UTC 29 May 1993	NMC analysis	0000 UTC 14 Dec 1988	NCEP reanalysis
0000 UTC 28 May 1994	NMC analysis	0000 UTC 13 Dec 1990	NCEP reanalysis
1200 UTC 28 May 1994	NMC analysis	1200 UTC 13 Dec 1990	NCEP reanalysis
0000 UTC 29 May 1994	NMC analysis	0000 UTC 14 Dec 1990	NCEP reanalysis

in all the integrations. The soil wetness and snow were predicted after initialization in both the AGCM and the nested Eta model by their respective parameterizations. Because the surface physics treatments in these two models are quite different, the initialization of the snow and soil wetness are not identical, but follow the same principles.

The snow cover in each model was initialized from seasonally varying climatological data. In the COLA AGCM the snow is initialized via an algorithm that derives daily snow cover and snow depth from the seasonal albedo data of Posey and Clapp (1954). In the Eta model the snow is initialized via an algorithm that derives daily snow cover and snow depth from a 1967–80 daily snow cover climatology calculated from the weekly National Environmental Satellite Data and Information Service snow–ice mask. The initial snow cover used in the AGCM and the nested Eta model were compared and were found to be quite similar.

All the integrations were initialized with observationally based soil wetness. The soil wetness used for initialization of the AGCM integrations was derived from the operational ECMWF analysis–forecast cycle soil moisture via an algorithm described by Fennessy and Shukla (1996). The 1987, 1988, and 1993 summer AGCM integrations were initialized with the ECMWF-derived soil wetness, and the 1986 and 1994 summer AGCM integrations and all the winter AGCM integrations were initialized with a 1987–93 climatology of the ECMWF-derived soil wetness. The nested Eta integrations were all initialized with NCEP reanalysis soil wetness obtained from the data archived at the National Center for Atmospheric Research (NCAR).

3. Seasonal mean climate hindcasts

To evaluate how the nested Eta model hindcasts compare to those from the AGCM alone, 15 member ensemble seasonal means, which are composed of three integrations from each of five different years, are examined (Table 1). These ensembles are compared to observations averaged over the same 5 yr. All figures show continental North America and the adjoining ocean areas, which is the main region of interest, rather than the whole domain, which is shown in Fig. 1. For the initial stage of analysis, examination of predicted fields confirmed that the AGCM and nested predictions match at the lateral boundaries.

a. Summer

The 5-yr mean JJAS 2-m temperature obtained from the Climate Anomaly Monitoring System (Ropelewski et al. 1985) station data is shown in Fig. 3a. The corresponding ensemble mean errors for the AGCM and the nested model are shown in Figs. 3b,c, respectively. The model temperatures are adjusted using a lapse rate of 6.5°C km^{-1} for the difference between the elevation of each model grid box and the mean elevation of the stations used to form the gridded observation. Both models have significant negative errors of 2°C or more over much of the continent, but the AGCM errors are larger, reaching 4°C or more over northern Alaska and Canada. However, the region of 1°C or more negative error in the nested model covers more of the continent than it does in the AGCM.

The observed 5-yr mean JJAS precipitation from a combination of station and satellite data (Xie and Arkin 1996) is shown in Fig. 4a. The corresponding ensemble mean AGCM and nested model precipitation is shown in Figs. 4b,c respectively. The superiority of the nested model in predicting precipitation is immediately evident. The AGCM prediction grossly overestimates the summer precipitation over much of the continent. The nested model correctly predicts the precipitation maxima over the northwest and eastern coastal areas, as well as the gradient across the central United States and the minima over the western United States (Fig. 4c). The main weakness in the nested model hindcasts is the less than observed precipitation over the far southeast United States, the Gulf of Mexico, and the Atlantic. Poor prediction of the North American summertime precipitation

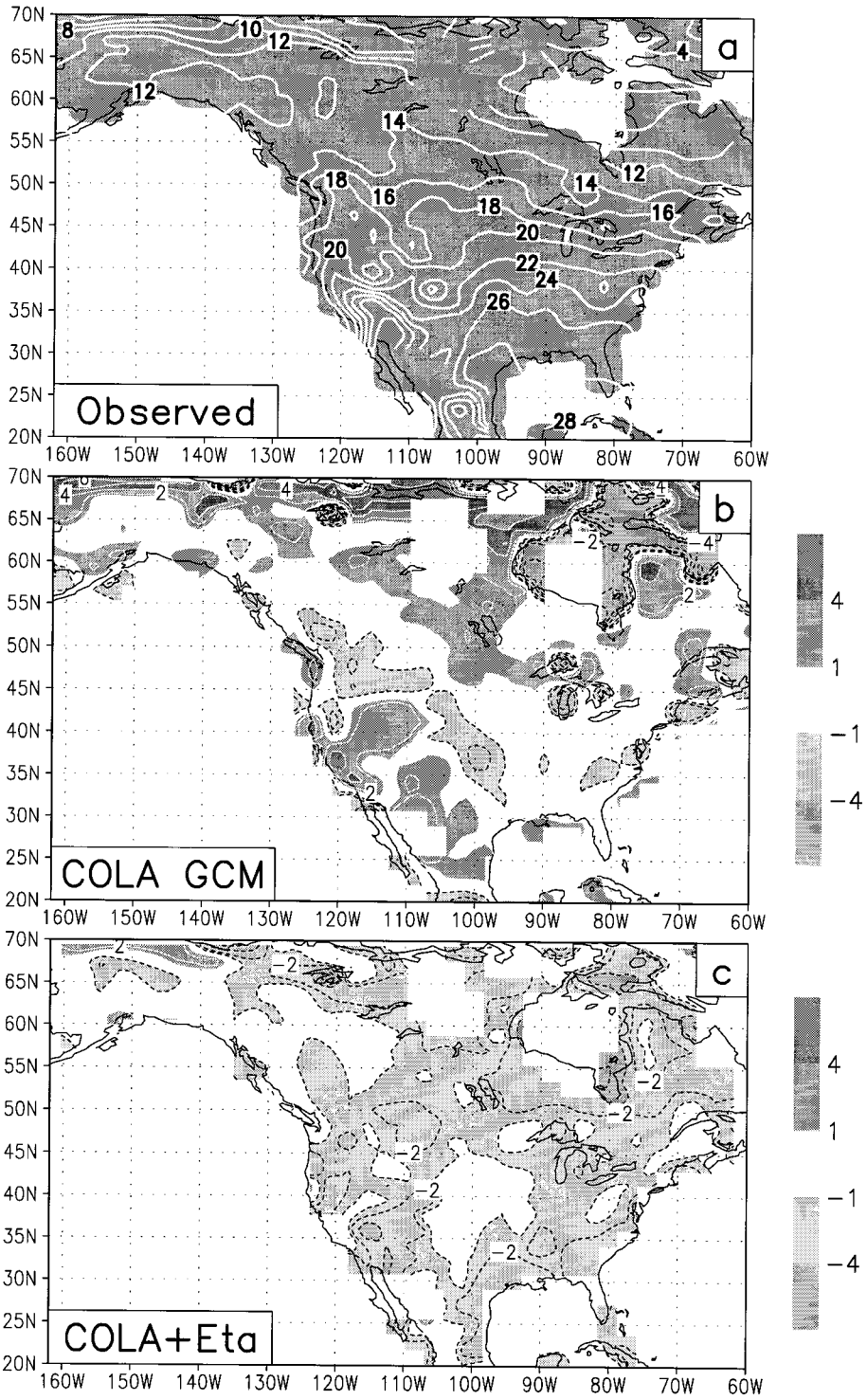

FIG. 3. JJAS 5-yr ensemble mean 2-m temperature for (a) observations (see text), (b) COLA AGCM error, and (c) nested Eta model error. Contour interval is 2°C in (a), contours are ±1°, 2°, 4°, 6°, 8°C in (b) and (c).

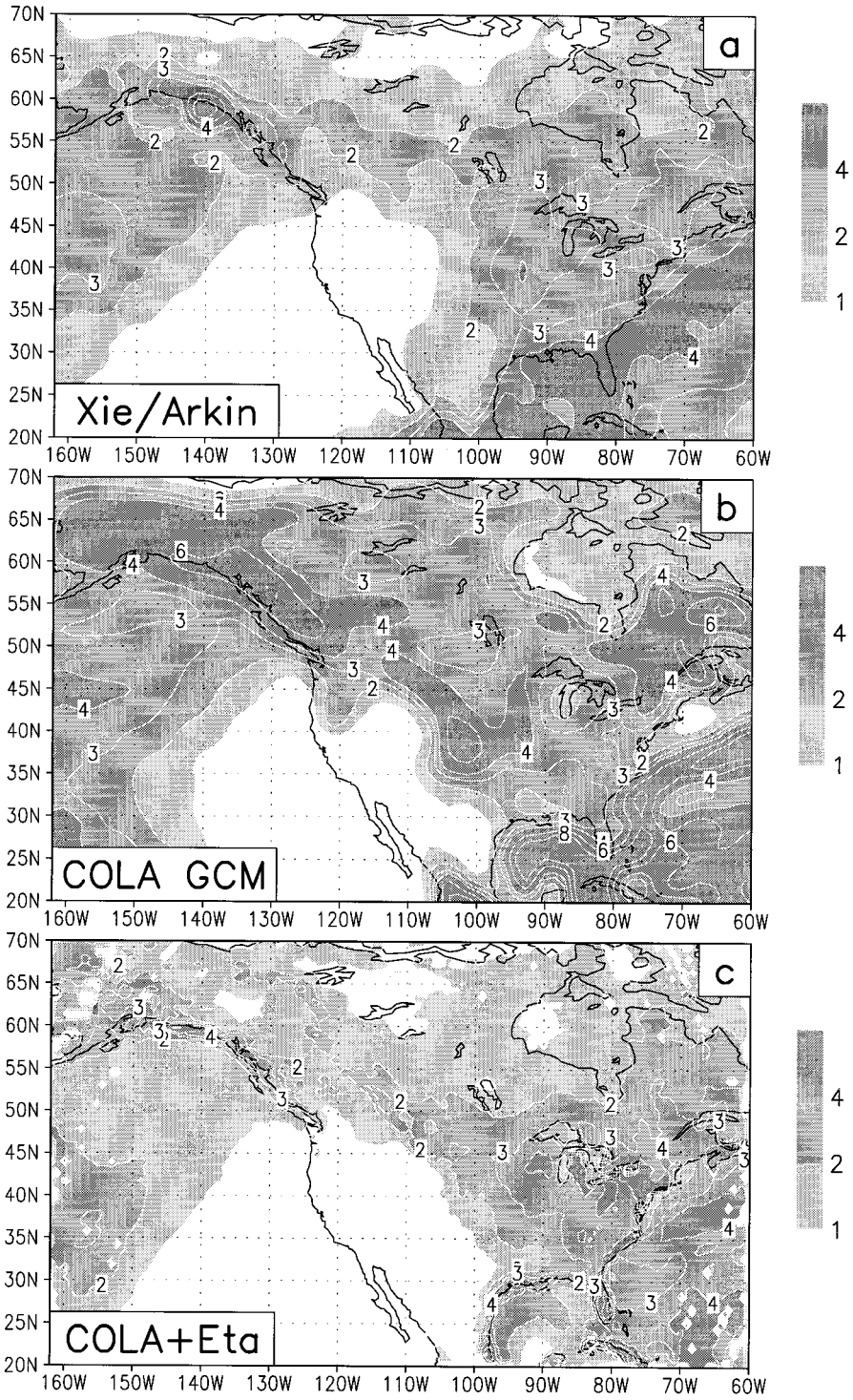

FIG. 4. JJAS 5-yr ensemble mean precipitation for (a) Xie/Arkin observations, (b) COLA AGCM, and (c) nested Eta model. Contours are 1, 2, 3, 4, 6, 8 mm day^{-1}.

is a common problem in many AGCMs. Similar deficiencies were found in an examination of the North American summer precipitation simulated by the NCEP T62 and NCAR Community Climate Model version 3 AGCMs (not shown).

Over the eastern United States both the COLA AGCM and the nested Eta model have reasonable simulations of the mean summer precipitation. Averaged over 35°–45°N and 75°–90°W the observed JJAS precipitation for these 5 yr is 3.0 mm day^{-1}, the AGCM is 2.9 mm day^{-1} and the nested Eta is 3.5 mm day^{-1}. The real problem in the COLA AGCM simulations but not in the nested Eta model simulations is the rainfall maximum to the west. Averaged over 35°–45°N, 95°–110°W the observed precipitation is 1.8 mm day^{-1}, the AGCM 4.1 mm day^{-1}, and the nested Eta 1.5 mm day^{-1}. This precipitation difference appears to be related to differences in the representation of orography and differences in the simulation of the low-level jet (LLJ). Recently, a strong link between the strength of the LLJ and summertime precipitation over the central United States was demonstrated by Higgins et al. (1997). Figure 5 shows (a) the ensemble mean JJAS mean nested Eta minus AGCM difference in precipitation, (b) the Eta minus AGCM orography difference, and (c) the 5 m s^{-1} contour of the ensemble mean JJAS mean 850-hPa meridional wind for observations (NCEP reanalysis, solid), AGCM (dashed), and nested Eta (dotted). The large greater than 4 mm day^{-1} negative difference in precipitation at 35°–45°N, 95°–105°W is adjacent to and downstream of large positive differences in model orography (up to 800 m). These differences occur due to the superior representation of the sharp height gradients of the front range of the Rockies in the Eta model. In the AGCM these gradients are smoothed out, as can be seen by careful inspection of Fig. 2a. The 5 m s^{-1} contour in Fig. 5c was arbitrarily chosen to represent the core of the LLJ. The AGCM 5 m s^{-1} contour (dashed curve) is not closed because the AGCM post processing does not extend below ground level. It is evident that both models simulate a LLJ, but that the LLJ in the AGCM is well westward of that observed. The LLJ in the nested Eta model is collocated with that observed, but extends more to the northeast. Within the core the nested Eta LLJ is also stronger than that observed (not shown). The AGCM has a poor simulation of where the jet enters from the Gulf at about 95°–100°W, 25°–30°N. Examination of longitude–pressure cross sections reveals that the LLJ in the AGCM is too shallow and the LLJ in the nested Eta model is too strong and deep compared to NCEP reanalysis (not shown). A feature that is evident in the reanalysis, AGCM, and nested Eta in Fig. 5c is the eastward turning of the LLJ in the vicinity of 35°–45°N, the importance of which has been noted by Giorgi and Shields (1999). Despite this turning, the AGCM LLJ remains well west of that observed (Fig. 5c). An examination of the low-level moisture convergence difference between the two models (not shown)

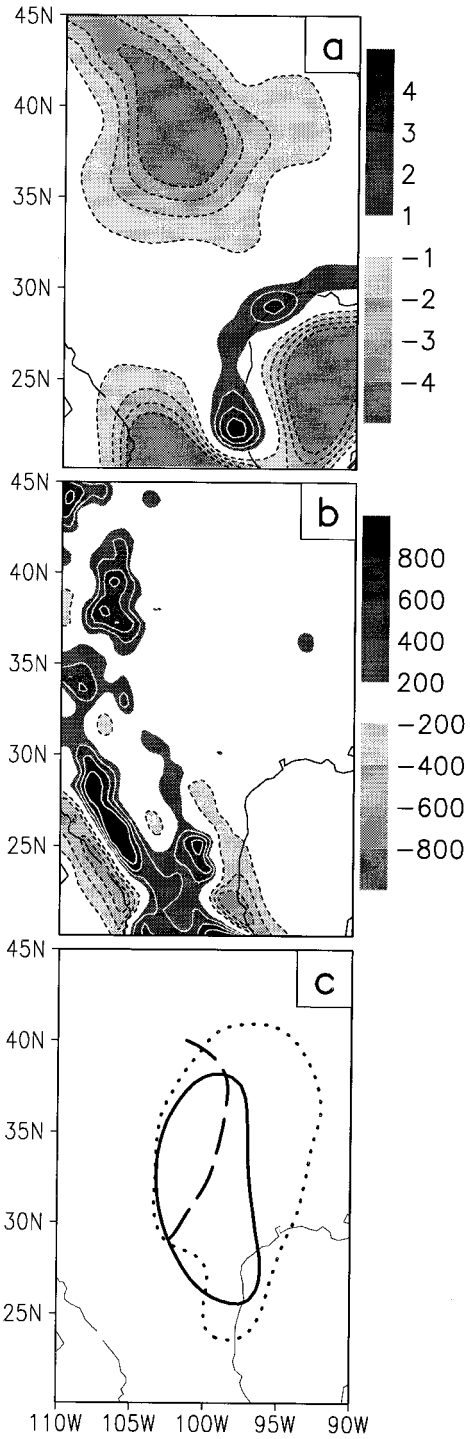

FIG. 5. Central United States (a) JJAS 5-yr ensemble mean precipitation difference for nested Eta model minus COLA AGCM, (b) nested Eta model minus COLA AGCM orography difference, and (c) JJAS 5-yr ensemble mean 5 m s^{-1} contour of the 850-hPa meridional wind for observations (solid), COLA AGCM (dashed), and nested Eta (dotted). Contours are (a) ±1, 2, 3, 4 mm day^{-1} and (b) ±200, 400, 600, 800 m.

shows that relative to the nested Eta model, the AGCM has considerably greater convergence of moisture in the central United States and considerably less in the eastern United States, supporting the idea that the westward displacement of the LLJ in the AGCM is at least partially responsible for its incorrect precipitation maximum. Following the work of McNider and Pielke (1981), concerning the importance of the orographic slope in correctly simulating the LLJ, we believe it is likely that the model differences in simulating the LLJ are at least partially due to the different representation of orography in the two models.

The predicted ensemble mean upper-level wind, height, and temperature fields have also been compared to observations, and in general, the AGCM and nested model error fields are quite similar (not shown). For example, relative to NCEP reanalyses, the AGCM 300-HPa geopotential height field has negative biases in the range of 60–90 m, whereas the nested model has broader negative biases in the range of 30–60 m.

b. Winter

The 5-yr mean JFM 2-m temperature obtained from the Ropelewski et al. (1985) station data is shown in Fig. 6a. The corresponding ensemble mean height corrected errors for the AGCM and the nested model are shown in Figs. 6b,c respectively. In general, the North American continent winter season surface temperature predictions of the two models have different, but large errors. Both models have significant positive errors of 4°C or more over the northern continent, but the AGCM errors are larger and extend southward into the central United States. The nested model negative bias over the eastern United States reaches 4°C or more whereas the AGCM negative bias in the same region is roughly half that magnitude. The 5-yr ensemble mean JFM mean nested Eta model minus COLA AGCM difference in 2-m temperature is shown in Fig. 7a. A large negative difference of up to 6°C in the nested model relative to the AGCM covers most of North America. To understand this difference, the cloudiness, snow, surface fluxes, and surface albedo in the two models have been compared. The total cloudiness is somewhat different between the two models but not in a systematic fashion that would contribute to the observed surface temperature differences (not shown). Differences in the surface fluxes of latent and sensible heat also do not appear to be systematic and/or related to the surface temperature biases, but interesting and systematic differences were found over ocean regions (not shown). In both seasons the nested Eta model had roughly 20 W m^{-1} less latent heat flux and 20 W m^{-1} more sensible heat flux over ocean regions than did the AGCM. This could be related to the tendency for the nested Eta model to have less precipitation over ocean regions than does the AGCM alone.

Figure 7 shows the JFM mean model differences in (b) surface albedo (fractional) and (c) snow depth (water equivalent, meters). The surface temperature differences (Fig. 7a) do appear to be strongly related to differences in the surface albedo in the two models. These differences are related to differences in both snow extent (cover and depth) and differences in the albedo over snow in the two models. Part of these differences are related to different initialization of snow in the two models. Both are initialized using derived climatological snow cover, which have different sources, but are very similar to each other. However, each model used a different algorithm to derive snow depth from the snow cover and the nested Eta model ends up with considerably deeper initial snow than does the COLA GCM. After initialization both models predict the snow depth and some of the differences may be due to differences in snow accumulation and melting between the two models. However, when comparing Figs. 7a and 7c it is clear that the region of significantly greater snow cover and depth persisting and/or evolving in the nested Eta model than in the AGCM alone is highly correlated with the region of greatest surface temperature differences between the two models. At least part of these differences could no doubt be eliminated by initializing both models with the same observed snow depth rather than by calculating the snow depth from the snow cover with an unrealistic algorithm. Some of the differences are likely related to different snow albedos used by the models, apparently higher in the Eta than in the COLA GCM. Mitchell (1999) has noted that the Eta model tends to have cold biases over snow and that the snow albedo used in the Eta model may be unrealistically high.

The observed 5-yr mean JFM precipitation (Xie and Arkin 1996) is shown in Fig. 8a. The corresponding ensemble mean AGCM and nested model precipitation is shown in Figs. 8b,c respectively. The AGCM overestimates the precipitation over much of the continent, though not as badly as it did in summer. The nested model correctly predicts the precipitation maxima over the northwest coast and the minima in the central continent. However, the northwest coast maxima is somewhat overestimated and the southeast United States and the gulf of Mexico maxima is underestimated. The AGCM also has a low bias over the southeast United States. Overall, the winter precipitation of the nested model is superior to that of the AGCM alone, but the differences between the AGCM and the nested model are not as large as they were in summer. The JFM ensemble mean errors in the upper-level wind, height, and temperature fields are very similar between the AGCM and nested model (not shown), and are larger in magnitude than those during summer.

4. Interannual variability

In order to be useful for practical climate applications, a nested model must be able to predict features of the

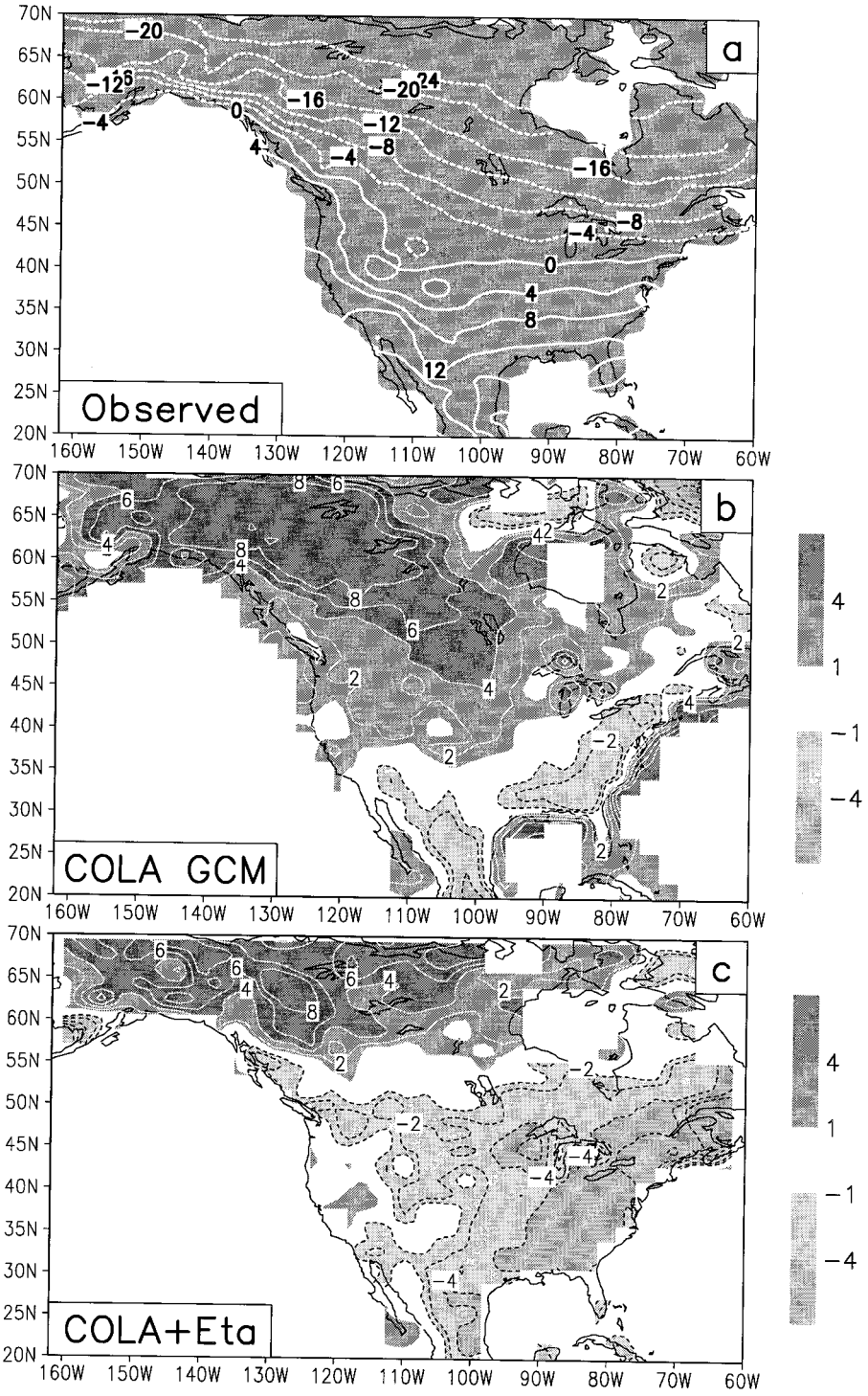

FIG. 6. JFM 5-yr ensemble mean 2-m temperature for (a) observations (see text), (b) COLA AGCM error, and (c) nested Eta model error. Contour interval is (a) 4°C, contours are (b), (c) ±1°, 2°, 4°, 6°, 8°C.

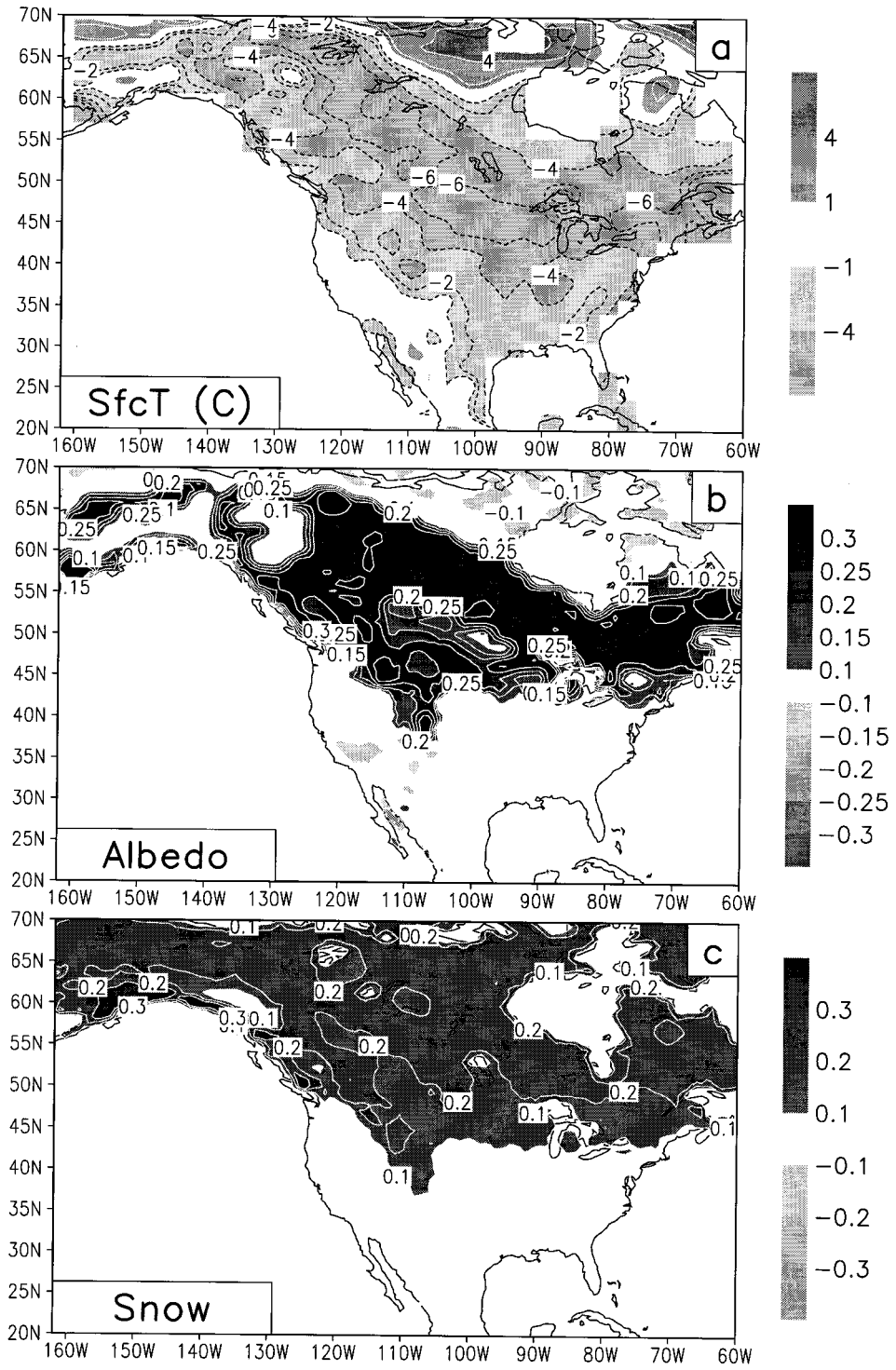

FIG. 7. JFM 5-yr ensemble mean nested Eta model minus COLA AGCM difference in (a) 2-m temperature, (b) surface albedo, and (c) snow depth. Contours are (a) ±1°, 2°, 4°, 6°, 8°C, (b) ±0.1, 0.15, 0.2, 0.25, 0.3, and (c) ±0.1, 0.2, 0.3.

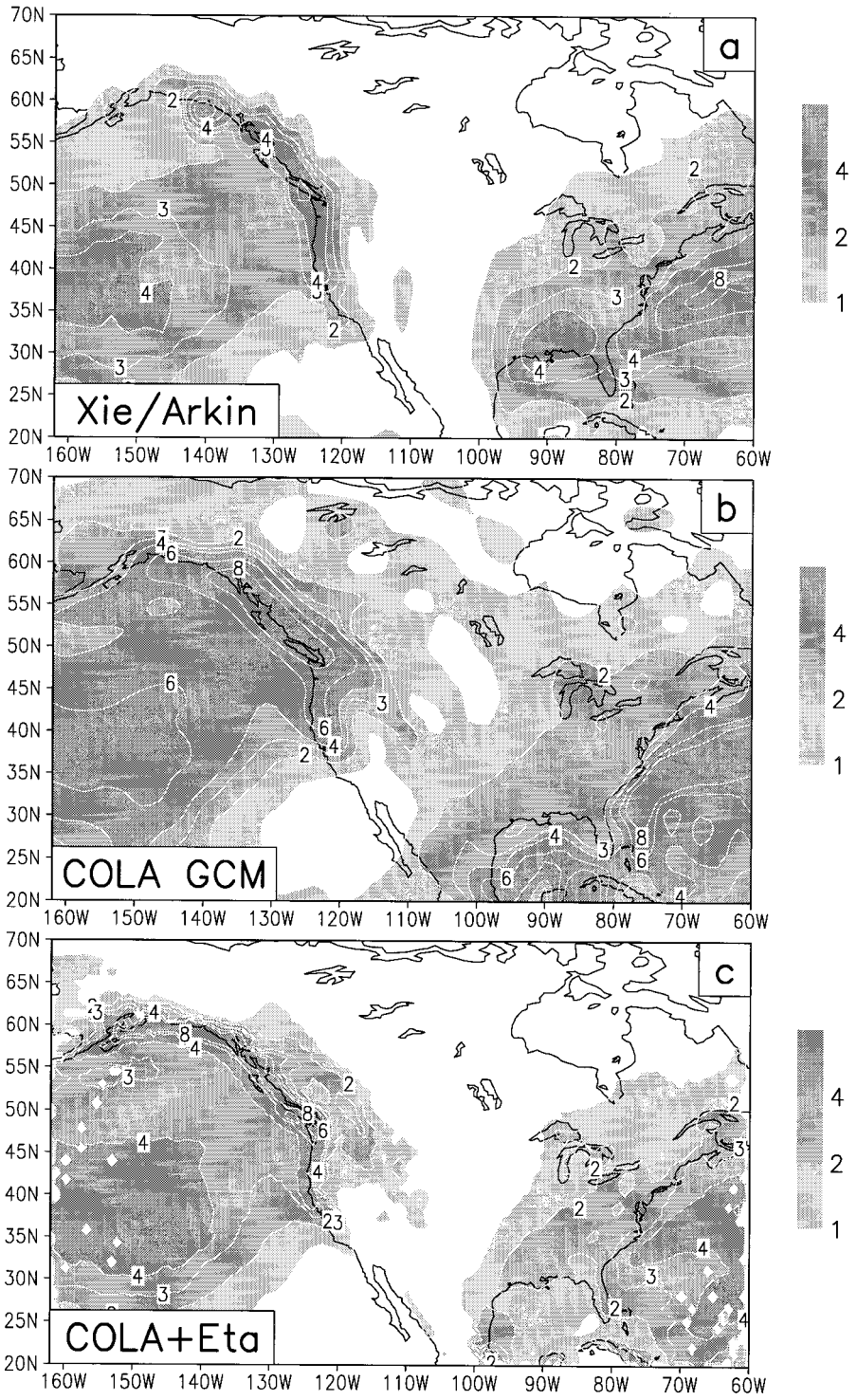

FIG. 8. JFM 5-yr ensemble mean precipitation for (a) Xie/Arkin observations, (b) COLA AGCM, and (c) nested Eta model. Contours are 1, 2, 3, 4, 6, 8 mm day^{-1}.

observed interannual variability that are due to either local boundary forcing, such as soil wetness or snow effects, or remote boundary forcing, such as SST effects, that are felt by the nested model through the lateral boundaries. The AGCM and nested model interannual variability was compared to the observed interannual variability. In general, the nested model interannual variability is similar and perhaps somewhat improved compared to that simulated by the AGCM alone. For the sake of brevity, only one summer and one winter case are presented in detail, chosen because of the large climate anomalies observed. The skill of the two models in general is compared by analyzing area-averaged systematic errors and rms errors for each year.

a. Summer

During April–June of 1988 low rainfall caused a severe drought in the corn belt of the central United States that left the region dry for the remainder of the summer. During June and July of 1993 persistent heavy rainfall caused severe flooding all along the Mississippi river basin. Although each of these two unconnected events had unique characteristics and life cycles, the difference between them is striking and presents a strong and important climatic signal that must be predicted by models that are to be used for climate prediction research. A brief summary of how the AGCM and nested models predicted this signal is presented here.

The 1993 versus 1988 lower boundary forcing differences for the AGCM and the nested model were nearly identical. The models had identical SST forcing (Reynolds and Smith 1994), and similar positive 1993 minus 1988 initial soil wetness differences in the corn belt of the United States (not shown).

The observed June–July mean 2-m temperature difference for 1993 minus 1988 obtained from station data (Ropelewski et al. 1985) is shown in Fig 9a. The corresponding three member ensemble mean temperature differences for the AGCM and the nested model are shown in Figs. 9b,c, respectively. Both models predict a large region of relatively colder temperature for 1993 in the central United States, though both center the region somewhat east of that observed and neither produces the observed magnitude (6°–8°C). Although the two model hindcasts are largely similar, the nested model better predicts the magnitude of the observed anomaly, reaching 4°C. The AGCM also extends the anomaly more southward than observed.

The observed June–July mean 1993 minus 1988 precipitation difference (Xie and Arkin 1996) is shown in Fig. 10a. The corresponding three member ensemble mean precipitation differences for the AGCM and the nested model are shown in Figs. 10b,c, respectively. Prominent in the observations is a broad 1 mm day^{-1} positive precipitation difference that spans much of the central United States and reaches over 4 mm day^{-1} over the upper Mississippi basin. The AGCM does not predict this signal at all, but rather has weaker positive differences both eastward and southward of the observed positive difference. The nested model does a far better job of predicting the broad 1 mm day^{-1} difference, though it extends it a bit too far southward and eastward. The nested model also properly places the center of the large difference over the corn belt with a maxima of over 3 mm day^{-1}, which is somewhat less than that observed. The surprising difference in the ability of the two models to predict this large and important signal merits further analysis. The upper-level circulation associated with this precipitation difference appears to be quite similar in the two models. Both models simulated similar large negative June–July 1993 minus 1988 differences in the 300-hPa geopotential height over the United States (90 m) that were weaker than the very large observed difference (150 m, not shown).

Figure 11 shows the 3-case mean June–July mean nested Eta simulation minus AGCM simulation of the 1993 minus 1988 precipitation difference. The corresponding June–July difference in the simulated 1993 minus 1988 evaporation difference is shown in Fig. 11b. There is a clear correspondence between most of the differences in Figs. 11a and 11b, indicating that differences in the simulated evaporation (Fig. 11b) contributed to the differences in the simulated precipitation (Fig. 11a). The large positive evaporation difference at 35°–45°N, 105°–95°W is collocated with the unrealistic JJAS precipitation maximum simulated by the AGCM (Fig. 4b), but not the nested Eta model (Fig. 4c), evident in the JJAS precipitation difference (Fig. 5a). The 2m s^{-1} contour of the observed June–July 1993 minus 1988 difference in meridional wind is shown in Fig. 11c. The corresponding AGCM and nested Eta 2 m s^{-1} difference contours are shown in Fig. 11c as dashed and dotted, respectively. The region where the observed June–July 1993 meridional wind exceeded that in 1988 by 2 m s^{-1} or more extends from the Gulf of Mexico at 90°–95°W, 20°N northward through the central United States and then northeast over the 1988 drought and 1993 flood areas. This difference represents the much stronger LLJ observed in 1993 than in 1988. Neither model does a good job of simulating this difference, but the nested Eta model at least simulates some of it, which resulted in moisture convergence differences (not shown) that contributed to the simulated precipitation differences in the 35°–45°N region. The corresponding AGCM differences in the LLJ resulted in additional moisture convergence (not shown) and precipitation along the coast in 1993 versus 1988 (Fig. 10b). Thus the difference in the two models' hindcasts of the observed 1993–1988 precipitation differences is related to their ability to simulate both the local evaporation and meridional flow differences. It appears likely that improvements in the nested Eta model (relative to the AGCM) in the simulation of the mean summer precipitation and the LLJ are responsible for its more realistic simulation of the 1993 minus 1988 differences. This is in agreement with

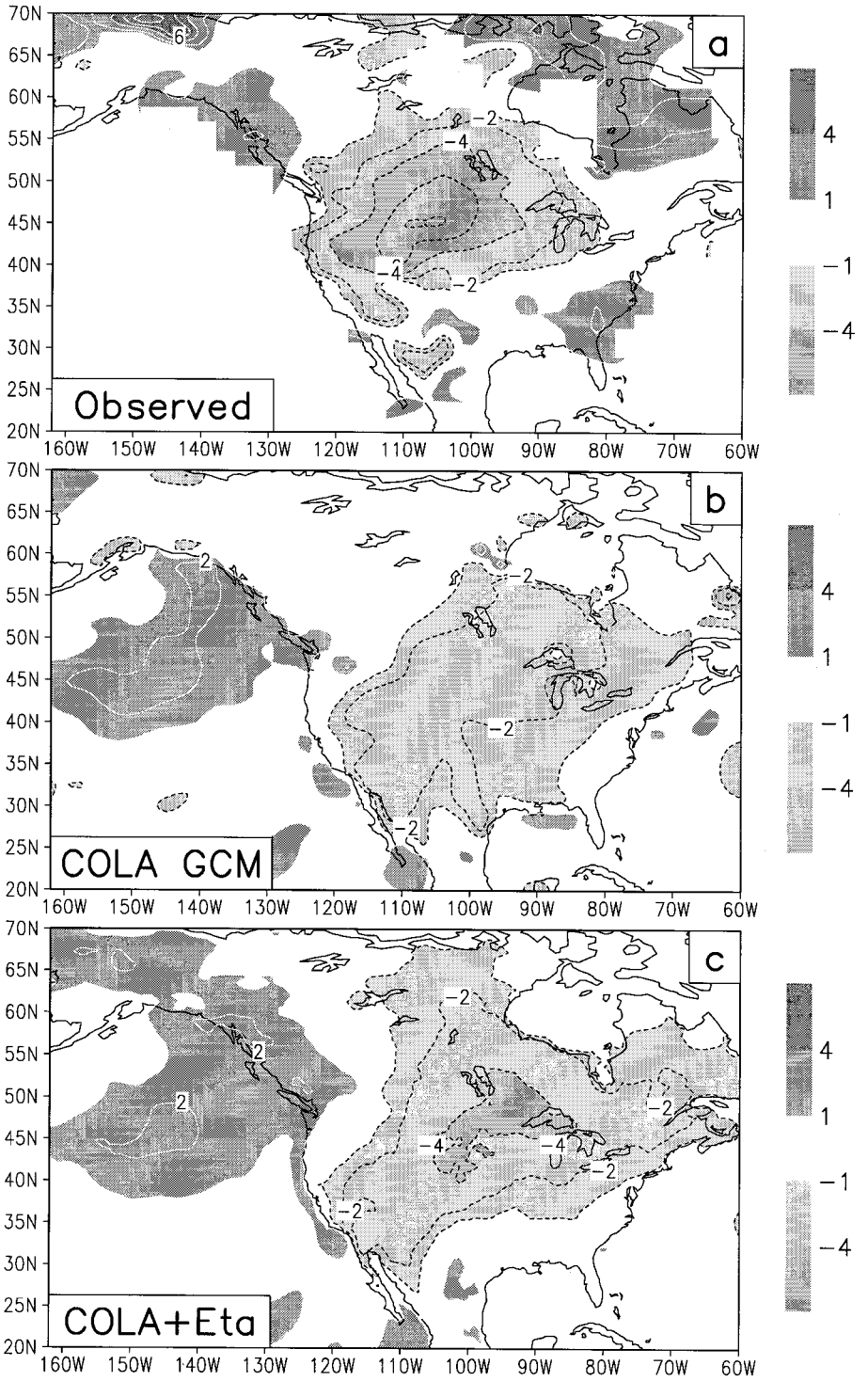

FIG. 9. Jun–Jul mean 1993 minus 1988 2-m temperature difference for (a) observations (see text), (b) COLA AGCM ensemble, and (c) nested Eta model ensemble. Contours are ±1°, 2°, 4°, 6°, 8°C.

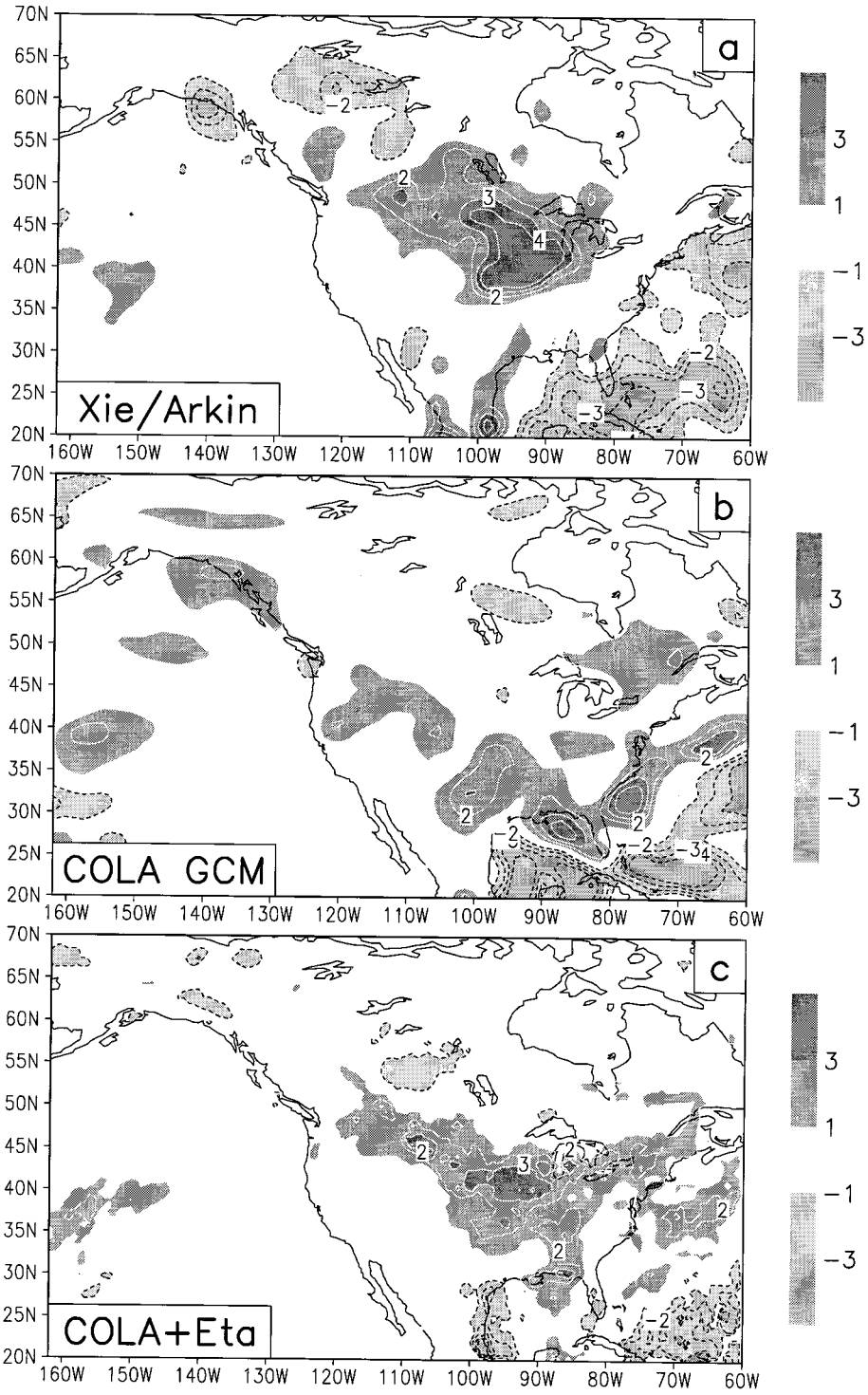

FIG. 10. Jun–Jul mean 1993 minus 1988 precipitation difference for (a) Xie/Arkin observations, (b) COLA AGCM ensemble, and (c) nested Eta model ensemble. Contours are ±1, 2, 3, 4 mm day^{-1}.

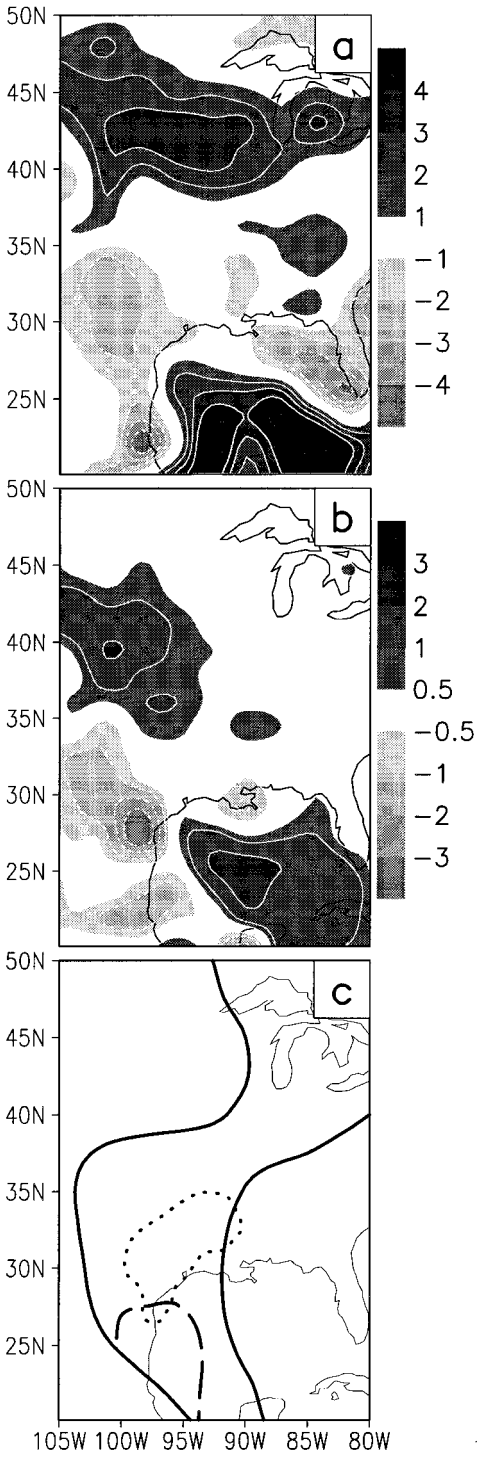

FIG. 11. Nested Eta model minus COLA AGCM difference of Jun–Jul mean 1993 minus 1988 difference for (a) precipitation and (b) evaporation. Contours are ±1, 2, 3, 4 mm day^{-1} in (a) and ±0.5, 1, 2, 3 mm day^{-1} in (b). (c) The 5 m s^{-1} contour of the Jun–Jul 1993 minus 1988 difference in the 850-hPa meridional wind for observations (solid), COLA AGCM (dashed), and nested Eta (dotted).

the results of Mo et al. 1995, who concluded that an anomalously strong LLJ was an essential ingredient in developing and maintaining the summer floods of 1993.

b. Winter

The winter years chosen in this study include 1982/83, which had large positive SST anomalies in the tropical Pacific accompanied by strong climate anomalies over North America, and 1988/89, which had large negative SST anomalies in the tropical Pacific. The winter of 1982/83 was warm over most of the United States, cold over much of Canada, and was wet along the west and southeast coasts. The winter of 1988/89 had much weaker anomalies over North America, thus differences between the 2 yr reflect mainly the strong 1982/83 anomalies.

The observed JFM 1989 minus JFM 1983 2-m surface temperature differences calculated from the Ropelewski et al. (1985) station data contain a broad region of large negative differences across the northern United States/southern Canada and a band of positive differences to the north (Fig. 12a). The AGCM (Fig. 12b) and the nested model (Fig. 12c) ensembles predict negative differences across the entire northeast half of the continent that are quite similar to each other, but quite different from the observed anomalies.

Both the AGCM (Fig. 13b) and the nested model (Fig. 13c) get reasonable predictions of the negative precipitation differences observed along the west and southeast coasts of the United States (Fig. 13a; Xie and Arkin 1996). Although they are generally similar, the differences predicted by the nested model contain more details than those predicted by the AGCM alone, particularly in regions with strong orographic features. However, one feature predicted by the AGCM but missed by the nested model is the positive difference that extends from south of the Great Lakes to Oklahoma in the observations.

c. Systematic error and root-mean-square error

To facilitate objective evaluation of the relative skills of the AGCM and the nested model, the seasonal mean systematic errors, rms errors, and anomaly correlations for hindcasts of 2-m temperature and precipitation have been calculated and area-averaged over the entire land surface area included in Figs. 3–13. The systematic errors are given in Table 2, the rms errors are given in Table 3, and the anomaly correlations are given in Table 4.

Both models exhibit large systematic temperature biases in both seasons. The AGCM is too warm relative to the observations in all 10 cases, and the nested model is too cold compared to observations in 9 of 10 cases. The AGCM temperature biases are larger in winter than in summer. The nested model biases are similar in magnitude in the two seasons. The nested model biases are

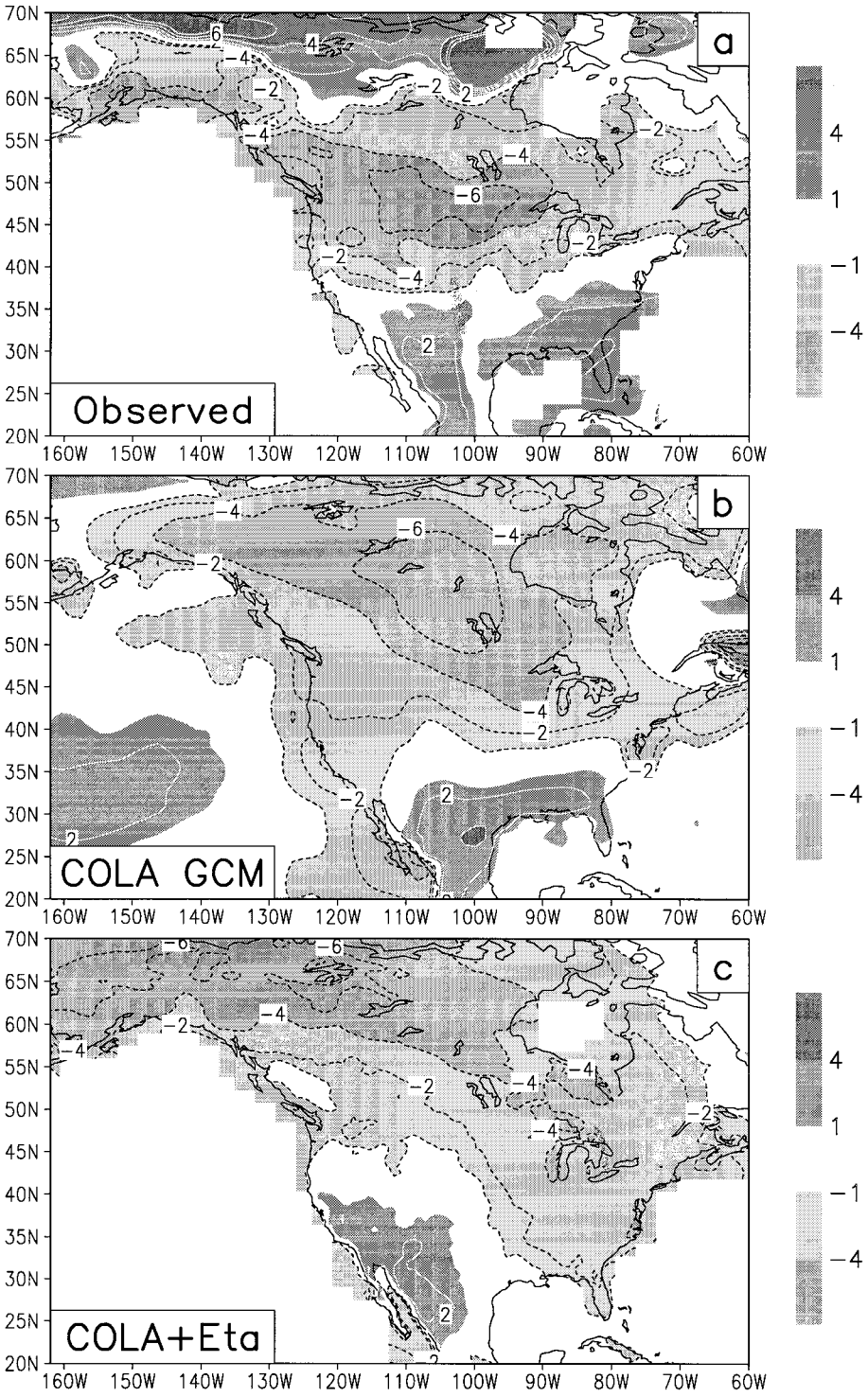

FIG. 12. JFM mean 1989 minus 1983 2-m temperature difference for (a) observations (see text), (b) COLA AGCM ensemble, and (c) nested Eta model ensemble. Contours are ±1°, 2°, 4°, 6°, 8°C.

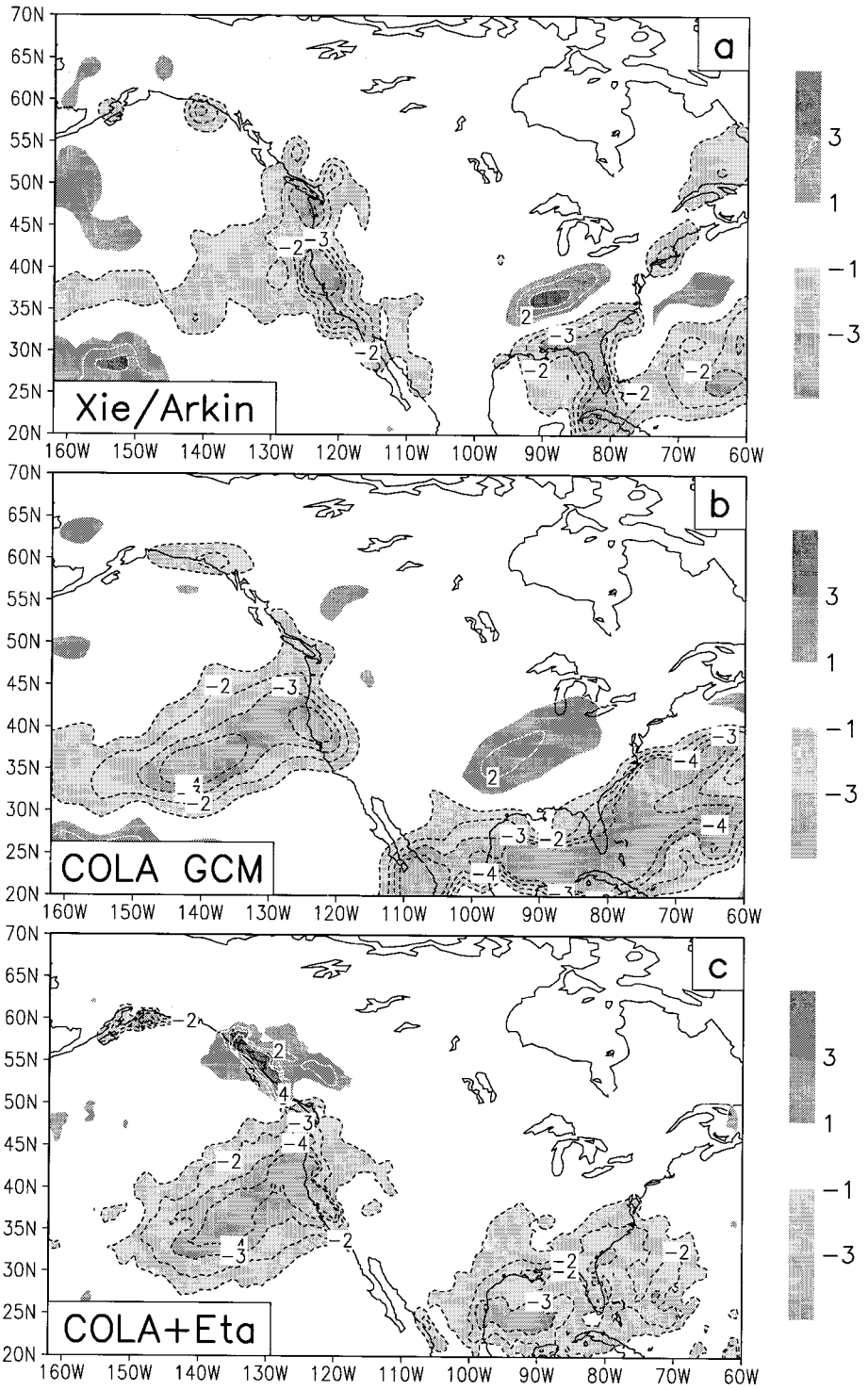

FIG. 13. JFM mean 1989 minus 1983 precipitation difference for (a) Xie/Arkin observations, (b) COLA AGCM ensemble, and (c) nested Eta model ensemble. Contours are ±1, 2, 3, 4 mm day^{-1}.

TABLE 2. Systematic error averaged over 20°–70°N, 162°–60°W, land only. Years for summer are 1986, 87, 88, 93, 94. Years for winter are 1983, 85, 87, 89, 91.

	Surface temperature (°C)				Precipitation (mm day^{-1})			
	Summer (JJAS)		Winter (JFM)		Summer (JJAS)		Winter (JFM)	
	COLA AGCM	COLA + Eta	COLA AGCM	COLA + Eta	COLA AGCM	COLA + Eta	COLA AGCM	COLA + Eta
Year 1	1.72	−0.84	3.23	0.35	0.95	−0.24	0.70	−0.04
Year 2	0.75	−1.65	2.40	−0.29	1.11	−0.13	0.59	−0.14
Year 3	0.91	−1.20	1.96	−1.63	1.13	−0.34	0.81	0.04
Year 4	0.67	−1.92	2.08	−1.06	1.03	−0.18	0.90	0.03
Year 5	0.83	−1.56	1.10	−1.35	1.22	−0.06	0.94	0.12
Mean	0.98	−1.43	2.15	−0.79	1.09	−0.19	0.79	0.00

larger (smaller) in magnitude than those of the AGCM alone in summer (winter).

Positive precipitation systematic biases of roughly 1 mm day^{-1} occur in the AGCM hindcasts in all the cases. The nested model has much smaller precipitation systematic biases, that are negative in most of the cases, but never exceed 0.34 mm day^{-1} in magnitude.

Due to the large systematic biases noted above, the area-average rms error in temperature is relatively large in both seasons and in both models. It is much larger in the winter season in both models (about 5°C), than in the summer season (about 2°C). This is likely due to the much larger temperature gradients and variability during the winter season, but may also be due in part to the positive impact of land surface processes on the summer temperature simulations. Overall, there is little difference in the rms error in temperature between the two models.

The AGCM precipitation rms error is between 1.9 and 2.1 mm day^{-1} in summer and between 1.4 and 1.7 mm day^{-1} in winter. The nested model precipitation rms error is between 0.9 and 1.2 mm day^{-1} in both seasons, which is considerably less than that of the AGCM alone.

The anomaly correlations for 2-m temperature and precipitation exhibit a large amount of interannual variability (Table 4). Over the entire 5 yr it does not appear that either model is the clear ''winner,'' although there is a tendency for the AGCM to score higher in winter and the nested model to score higher in summer.

The calculations presented in Tables 2, 3, and 4 confirm the impressions gained from examination of Figs. 3–8, that the 2-m temperature predictions of both the models are poor, and the predictions of precipitation by the nested model are significantly better than those by the AGCM alone.

5. Signal-to-noise calculations

From an analysis of the seasonal mean anomalies predicted by both models (including those discussed in the previous section) it appears that the nested model is capable of predicting most of the anomalies simulated by the AGCM alone and in some cases is capable of enhancing them or even predicting anomalies missed by the AGCM. From a wealth of climate studies with AGCMs it is well known that ensembles of predictions are required in order to obtain some measure of the significance and reliability of climate predictions. An important question is whether the ensemble size required for nested models is similar or different from that required for AGCMs alone. Although the ensemble sizes used in this preliminary study are modest, an attempt is made to shed light on this question by analyzing the interannual climate signal, the intraensemble noise, and the signal-to-noise ratios of the nested model hindcasts in comparison to those in the AGCM alone hindcasts. Despite the small ensemble size, the comparison between the AGCM and nested model results is useful because the calculation is done in an identical fashion for both.

TABLE 3. Rms error averaged over 20°–70°N, 162°–60°W, land only. Years for summer are 1986, 87, 88, 93, 94. Years for winter are 1983, 85, 87, 89, 91.

	Surface temperature (°C)				Precipitation (mm day^{-1})			
	Summer (JJAS)		Winter (JFM)		Summer (JJAS)		Winter (JFM)	
	COLA AGCM	COLA + Eta	COLA AGCM	COLA + Eta	COLA AGCM	COLA + Eta	COLA AGCM	COLA + Eta
Year 1	2.83	1.58	5.86	4.87	1.86	0.95	1.71	0.99
Year 2	2.25	2.24	4.68	4.29	1.87	0.93	1.41	1.05
Year 3	2.20	1.99	4.58	4.39	1.93	1.07	1.53	0.90
Year 4	1.95	2.35	4.89	4.11	1.97	1.16	1.51	1.20
Year 5	1.95	2.18	3.92	5.03	2.10	0.97	1.62	1.02
Mean	2.24	2.07	4.79	4.54	1.95	1.02	1.56	1.03

TABLE 4. Anomaly correlation averaged over 20°–70°N, 162°–60°W, land only. Years for summer are 1986, 87, 88, 93, 94. Years for winter are 1983, 85, 87, 89, 91.

	Surface temperature				Precipitation			
	Summer (JJAS)		Winter (JFM)		Summer (JJAS)		Winter (JFM)	
	COLA AGCM	COLA + Eta	COLA AGCM	COLA + Eta	COLA AGCM	COLA + Eta	COLA AGCM	COLA + Eta
Year 1	−0.08	0.22	0.09	0.01	0.11	−0.10	0.64	0.65
Year 2	0.09	−0.23	0.25	0.04	0.10	−0.13	0.49	0.58
Year 3	0.40	0.61	0.72	0.59	0.28	0.48	0.20	0.11
Year 4	0.52	0.71	0.47	0.20	−0.15	0.25	0.42	0.11
Year 5	0.66	0.55	0.25	0.03	−0.10	−0.04	0.08	−0.09
Mean	0.32	0.37	0.36	0.17	0.05	0.09	0.37	0.27

The ''signal''-to-''noise'' ratio σ_S^2/σ_N^2, is defined as the ratio between the interannual seasonal mean signal given by Eq. (1),

$$\sigma_S^2 = \sum_{j=1}^{m} (E_j - C)^2/(m - 1) - (1/n)\sigma_N^2 \qquad (1)$$

and the intraensemble seasonal mean noise given by Eq. (2),

$$\sigma_N^2 = \sum_{j=1}^{m} \frac{\left[\sum_{i=1}^{n} (r_{ij} - E_j)^2/(n - 1)\right]}{m}, \qquad (2)$$

where i is an individual member (of the $n = 3$ size ensemble) for a given year j (of $m = 5$ total years), and E_j is the model ensemble for a given year j, given by Eq. (3),

$$E_j = \sum_{i=1}^{n} \frac{r_{ij}}{n}, \qquad (3)$$

and r_{ij} is integration i of the ensemble for year j. The 5-yr mean ensemble C, is given by Eq. (4):

$$C = \sum_{j=1}^{m} \frac{E_j}{m}. \qquad (4)$$

The term on the right-hand side of Eq. (1) is a correction to account for the internal variability present in the ensemble mean for each year, due to sample size (Rowell et al. 1995). An examination of σ_S^2, σ_N^2, and σ_S^2/σ_N^2 for the AGCM and the nested model predictions for the 2-m temperature and precipitation fields shows that the signal and noise fields appear quite similar between the AGCM and the nested model. Differences show up better in the signal-to-noise ratio. The JJAS (JFM) signal-to-noise ratios of the 2-m temperature and precipitation are shown in Fig.14 (15) for land areas only. In each figure there are four frames: (a) AGCM temperature, (b) nested model temperature, (c) AGCM precipitation, and (d) nested model precipitation.

In general, the signal-to-noise ratios between the AGCM and the nested model are similar for a given field and season. In both seasons the signal-to-noise ratio is generally larger in magnitude and more spatially coherent for temperature than for precipitation. Also, in general, the summer (JJAS) signal-to-noise ratios of both temperature and precipitation have maxima in the central continent, and the winter (JFM) signal-to-noise ratio maxima are more widespread, with some tendency toward coastal areas. This is consistent with the role of land surface processes on atmospheric predictability, which is more prominent in the interior of continents and in the summer season (Karl 1983). It is also consistent with the positive impact of SST anomalies on predictability, which is more prominent along the coasts and during the winter season (Ropelewski and Halpert 1989, 1996).

The limited sample size prohibits careful analysis of the detailed differences between the AGCM and nested model fields. However, it does appear that in the winter season the nested model tends to have larger signal-to-noise ratios in both temperature and precipitation than does the AGCM alone. In summer the two models are quite similar, though the AGCM temperature signal-to-noise ratios are higher over the southeastern United States than are the nested models'. The most important point to note is the fact that the signal-to-noise ratios of the nested model are in general not less than those of the AGCM alone, despite the smaller scales resolved by the nested model.

6. Conclusions

An examination of 15 North American seasonal winter and summer hindcasts with the NCEP Eta model nested in the COLA AGCM shows that the nested model reduces the systematic errors in seasonal mean precipitation compared to the AGCM alone, and retains the interannual variability present in the AGCM predictions. The simulation of both the finer-scale details and the overall seasonal mean precipitation pattern were improved in the nested model. An examination of several other atmospheric variables showed that the nested model predictions were generally as good or better than those from the AGCM alone. The interannual variability was not only conveyed from the AGCM to the nested model, but was improved in some cases. It is not apparent whether the cause for this improvement was the different

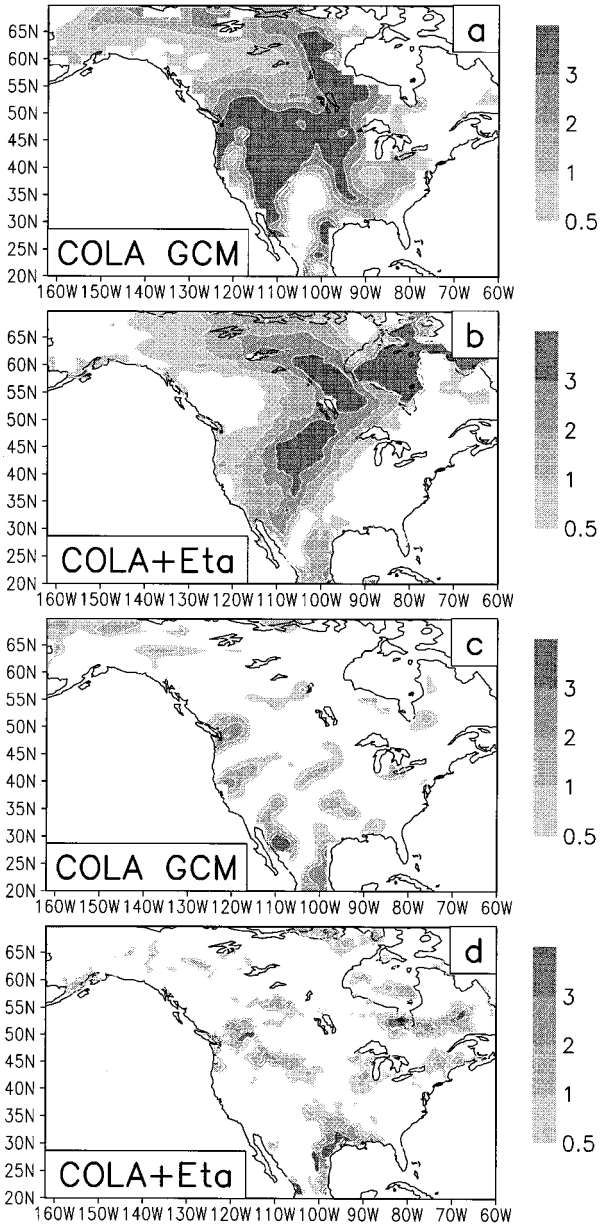

FIG. 14. JFM signal-to-noise ratio (see text) for (a) COLA AGCM 2-m temperature, (b) nested Eta model 2-m temperature, (c) COLA AGCM precipitation, and (d) nested Eta model precipitation.

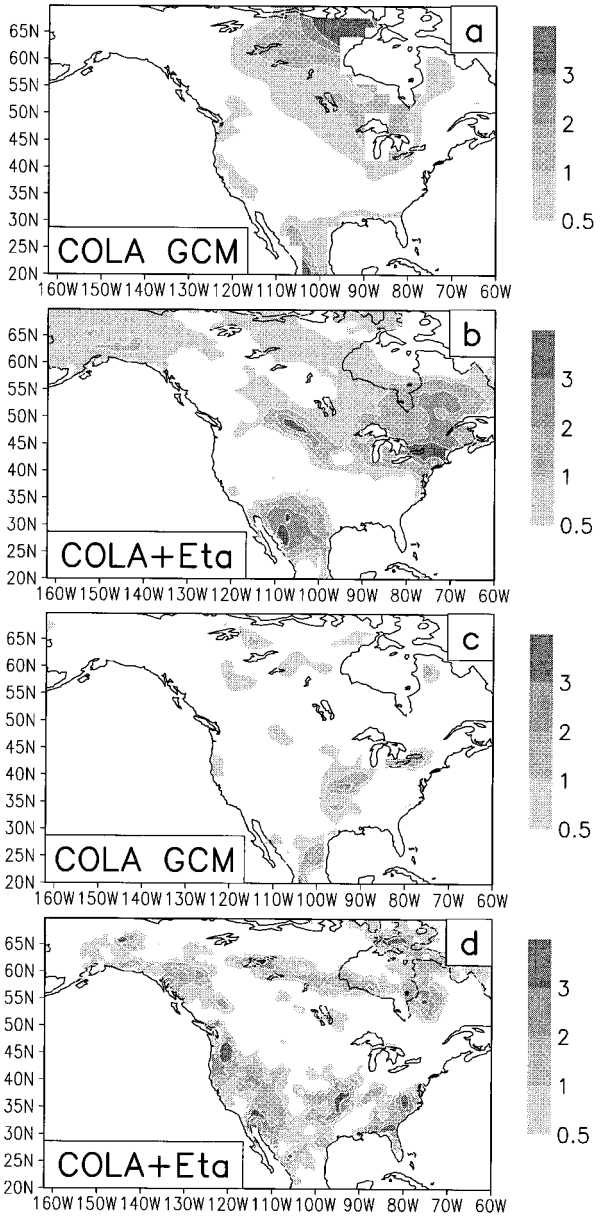

FIG. 15. JJAS signal-to-noise ratio (see text) for (a) COLA AGCM 2-m temperature, (b) nested Eta model 2-m temperature, (c) COLA AGCM precipitation, and (d) nested Eta model precipitation.

physics, the enhanced resolution, or the better representation of orography in the nested model, or some combination of the three. In particular the precipitation difference between the 1988 U.S. drought and 1993 U.S. flood was much better predicted by the nested model.

In addition to getting a reasonable prediction of the seasonal mean precipitation, it is important for regional applications that a model correctly predict the intraseasonal variability, particularly for precipitation. In a companion study, Shukla et al. (1997) have examined the AGCM and nested model simulations of the daily precipitation variability over different regions of the United States and found that the nested model had a more realistic intraseasonal variability compared to the AGCM alone. Those results, in combination with the results presented here, make it clear that the nested model captures both the mean precipitation and the precipitation variability better than the AGCM alone.

Despite the relatively small sample size, an attempt was made to make an estimate of the signal-to-noise characteristics of the nested predictions compared to that of the AGCM predictions. The signal, noise, and signal-to-noise-ratios of the near-surface temperature and pre-

cipitation fields were generally similar between the nested model and AGCM alone predictions. However, in the winter season the nested model tends to have larger signal-to-noise ratios in both temperature and precipitation compared to the AGCM alone. This result was somewhat unexpected because classical studies on the scale dependance of predictability suggest that a higher resolution model should allow errors in smaller-scale features to grow faster and generate a higher level of noise. If these results are valid for other cases, it could be concluded that the ensemble size required for predictions using nested models may not be larger than that required for AGCMs alone.

This study should be viewed in the context of the larger problem of regional climate prediction and assessment. These results are encouraging as they show that it is possible to go from seasonal predictions of planetary waves using an AGCM to predictions of regional precipitation using a regional model. In a future study, we propose to go on to the next step of driving even smaller-scale models of hydrology and water management using outputs of the nested regional model.

Acknowledgments. The authors would like to thank Y. Ji and E. Altshuler for help with technical aspects of the model simulations and T. Black, K. Mitchell, F. Mesinger, and Z. Janjic for useful discussions on aspects of the Eta model. The authors would also like to thank the anonymous reviewers for their constructive suggestions. All the Eta model calculations were done on NASA Center for Computational Sciences computers at Goddard Space Flight Center. This research was supported by NOAA Grant NA-76-GP0258, NASA Grants NAGW-1269 and NAGW-2661, and by NSF Grant ATM-90-19296.

REFERENCES

Alpert, J. C., M. Kanamitsu, P. M. Caplan, J. G. Sela, G. H. White, and E. Kalnay, 1988: Mountain induced gravity wave drag parameterization in the NMC medium-range forecast model. *Proc. Eighth Conf. on Numerical Weather Prediction*, Boston, MA, Amer. Meteor. Soc., 726–733.

Arakawa, A., and W. H. Schubert, 1974: Interaction of cumulus cloud ensemble with the large-scale environment. *J. Atmos. Sci.,* **31,** 671–701.

——, and V. R. Lamb, 1977: Computational design of the basic dynamical processes of the UCLA general circulation model. *Methods Comput. Phys.,* **17,** 173–265.

Betts, A. K., and M. T. Miller, 1986: A new convective adjustment scheme. Part II: Single column tests using GATE wave, BOMEX, and Arctic air-mass data. *Quart. J. Roy. Meteor. Soc.,* **112,** 693–703.

Black, T., 1994: The new NMC mesoscale Eta model: Description and forecast examples. *Wea. Forecasting,* **9,** 265–278.

Chen, F., Z. Janjic, and K. Mitchell, 1997: Impact of atmospheric surface layer parameterization in the new land-surface scheme of the NCEP mesoscale ETA numerical model. *Bound.-Layer Meteor.,* **85,** 391–421.

DeWitt, D. G., 1996: The effect of cumulus convection on the climate of COLA general circulation model. COLA Tech. Rep. 27, 43 pp. [Available from Center for Ocean-Land-Atmosphere Studies, 4041 Powder Mill Road, Suite 302, Calverton, MD 20705.]

Dorman, J. L., and P. Sellers, 1989: A global climatology of albedo, roughness length and stomatal resistance for atmospheric general circulation models as represented by the Simple Biosphere Model (SiB). *J. Appl. Meteor.,* **28,** 833–855.

Fels, S. B., and M. D. Schwarzkopf, 1975: The simplified exchange approximation: A new method for radiative transfer calculations. *J. Atmos. Sci.,* **32,** 1475–1488.

Fennessy, M. J., and J. Shukla, 1996: Impact of initial soil wetness on seasonal atmospheric prediction. COLA Tech. Rep. 34, 25 pp. [Available from Center for Ocean–Land–Atmosphere Studies, 4041 Powder Mill Road, Suite 302, Calverton, MD 20705.]

——, and Y. Xue, 1997: Impact of USGS vegetation map on GCM simulations over the United States. *Ecol. Appl.,* **7,** 22–23.

Giorgi, F., 1990: Simulation of regional climate using a limited area model nested in a general circulation model. *J. Climate,* **3,** 941–963.

——, and G. T. Bates, 1989: The climatological skill of a regional model over complex terrain. *Mon. Wea. Rev.,* **117,** 2325–2347.

——, and C. Shields, 1999: Tests of precipitation parameterizations available in latest version of NCAR regional climate model (RegCM) over continental United States. *J. Geophys. Res.,* **104,** 6353–6375.

Harshvardhan, R. Davies, D. A. Randall, and T. G. Corsetti, 1987: A fast radiation parameterization for general circulation models. *J. Geophys. Res.,* **92,** 1009–1016.

Higgins, R. W., Y. Yao, E. S. Yarosh, J. E. Janowiak, and K. C. Mo, 1997: Influence of the Great Plains low-level jet on summertime precipitation and moisture transport over the central United States. *J. Climate,* **3,** 481–507.

Hogan, T. F., and T. E. Rosmond, 1991: The description of the Navy operational global atmospheric prediction system's spectral forecast model. *Mon. Wea. Rev.,* **119,** 1786–1815.

Hou, Y.-T., 1990: Cloud–radiation–dynamics Interaction. Ph.D. dissertation, University of Maryland, College Park, 209 pp. [Available from University Microfilm, University of Maryland, College Park, MD 20742.]

Janjic, Z. I., 1984: Nonlinear advection schemes and energy cascade on semi-staggered grids. *Mon. Wea. Rev.,* **112,** 1234–1245.

——, 1990: The step-mountain coordinate: Physical package. *Mon. Wea. Rev.,* **118,** 1429–1443.

——, 1994: The step-mountain Eta coordinate model: Further developments of convection, viscous sublayer, and turbulence closure schemes. *Mon. Wea. Rev.,* **122,** 927–945.

Ji, Y., 1996: Modeling the Asian summer monsoon with high resolution regional Eta model: The impact of sea surface temperature anomaly associated with ENSO cycle. Ph.D. dissertation, University of Maryland, College Park, 139 pp. [Available from University Microfilm, University of Maryland, College Park, MD 20742.]

——, and A. D. Vernekar, 1997: Simulation of the Asian summer monsoons of 1987 and 1988 with a regional model nested in a global GCM. *J. Climate,* **10,** 1965–1979.

Karl, T. R., 1983: Some spatial characteristics of drought duration in the United States. *Climate Appl. Meteor.,* **22,** 1356–1366.

Kinter, J. L., III, J. Shukla, L. Marx, and E. K. Schneider, 1988: A simulation of the winter and summer circulations with the NMC global spectral model. *J. Atmos. Sci.,* **45,** 2486–2522.

——, and Coauthors, 1997: The COLA atmosphere–biosphere general circulation model. Vol. 1, Formulation. COLA Tech. Rep. 51, 44 pp. [Available from Center for Ocean-Land-Atmosphere Studies, 4041 Powder Mill Road, Suite 302, Calverton, MD 20705.]

Lacis, A. A., and J. E. Hansen, 1974: A parameterization for the absorption of solar radiation in the earth's atmosphere. *J. Atmos. Sci.,* **31,** 118–133.

Lobocki, L., 1993: A procedure for the derivation of surface-layer bulk relationships from simplified second-order closure models. *J. Appl Meteor.,* **32,** 126–138.

McNider, R. T., and R. A. Pielke, 1981: Diurnal boundary layer development over sloping terrain. *J. Atmos. Sci.,* **38,** 2198–2212.

Mellor, G. L., and T. Yamada, 1982: Development of a turbulence closure model for geophysical fluid problems. *Rev. Geophys. Space Phys.,* **20,** 851–875.

Mesinger, F., 1984: A blocking technique for representation of mountains in atmospheric models. *Riv. Meteor. Aeronaut.,* **44,** 195–202.

——, 1995: The eta regional model and its performance at the U.S. National Centers for Environmental Prediction. *Int. Workshop on Limited-Area and Variable Resolution Models,* Beijing, China, World Meteorological Organization, 19–28.

——, 1996: Improvements in quantitative precipitation forecasts with the Eta regional model at the National Centers for Environmental Prediction: The 48-km upgrade. *Bull. Amer. Meteor. Soc.,* **77,** 2637–2649.

——, and T. L. Black, 1992: On the impact of forecast accuracy of the step-mountain (eta) s. sigma coordinate. *Meteor. Atmos. Phys.,* **50,** 47–60.

——, Z. I. Janjic, S. Nickovic, D. Gavrilov, and D. G. Deaven, 1988: The step-mountain coordinate: Model description and performance for cases of Alpine lee cyclogenesis and for a case of an Appalachain redevelopment. *Mon. Wea. Rev.,* **116,** 1493–1518.

Mitchell, K., 1999: Cold bias in 2-m air temperature over snowcover in Eta model. EMC: Eta ''tip of the month.'' [Available online at http://nic.fb4.noaa.gov:8000/research/meso.tip.html.]

Miyakoda, K., and J. Sirutis, 1977: Comparative integrations of global spectral models with various parameterized processes of subgrid scale vertical transports. *Beitr. Phys. Atmos.,* **50,** 445–447.

Mo, K. C., J. Nogues-Paegle, and J. Paegle, 1995: Physical mechanisms of the 1993 summer floods. *J. Atmos. Sci.,* **52,** 879–895.

Moorthi, S., and M. J. Suarez, 1992: Relaxed Arakawa–Schubert: A parameterization of moist convection for general circulation models. *Mon. Wea. Rev.,* **120,** 978–1002.

Philips, N. A., 1957: A coordinate system having some special advantages for numerical forecasting. *J. Meteor.,* **14,** 184–185.

Posey, J. W., and P. F. Clapp, 1954: Global distribution of normal surface albedo. *Geofisica Int.,* **4,** 33–48.

Reynolds, R. W., and T. M. Smith, 1994: Improved global sea surface temperature analyses using optimum interpolation. *J. Climate,* **7,** 929–948.

Rogers E., D. G. Deaven, and G. J. DiMego, 1995: The regional analysis system for the operational ''early'' Eta model: Original 80-km configuration and recent changes. *Wea. Forecasting,* **10,** 810–825.

——, T. L. Black, D. G. Deaven, G. J. DiMego, Q. Zhao, M. Baldwin, N. W. Junker, and Y. Lin, 1996: Changes to the operational ''early'' Eta analysis/forecast system at the National Centers for Environmental Prediction. *Wea. Forecasting,* **11,** 391–413.

Ropelewski, C. F., and M. F. Halpert, 1989: Precipitation patterns associated with the high index phase of the Southern Oscillation. *J. Climate,* **2,** 268–284.

——, and ——, 1996: Quantifying Southern Oscillation-precipitation regimes. *J. Climate,* **9,** 1043–1059.

——, J. E. Janowiak, and M. F. Halpert, 1985: The analysis and display of real time surface climate data. *Mon. Wea. Rev.,* **113,** 1101–1107.

Rowell, D. P., C. K. Folland, K. Maskell, and M. N. Ward, 1995: Variability of summer rainfall over tropical north Africa (1906–92): Observations and modeling. *Quart. J. Roy. Meteor. Soc.,* **121,** 669–704.

Sato, N., P. J. Sellers, D. A. Randall, E. K. Schneider, I. Shukla, J. L. Kinter III, Y-T. Hou, and E. Albertazzi, 1989: Effects of implementing the Simple Biosphere Model in a general circulation model. *J. Atmos. Sci.,* **46,** 2757–2782.

Sela, J. G., 1980: Spectral modeling at the National Meteorological Center. *Mon. Wea. Rev.,* **108,** 1279–1292.

Sellers, P. J., Y. Mintz, Y. C. Sud, and A. Dalcher, 1986: A simple biosphere model (SiB) for use within general circulation models. *J. Atmos. Sci.,* **43,** 505–531.

Shukla, J., 1998: Predictability in the midst of chaos: A scientific basis for climate forecasting. *Science,* **282,** 728–731.

——, and Coauthors, 1997: A forecast of precipitation and surface air temperature in North America for winter (JFM) 1998. COLA Tech. Rep. 50, 11 pp. [Available online from Center for Ocean–Land–Atmosphere Studies, 4041 Powder Mill Road, Suite 302, Calverton MD 20705.]

Slingo, J. M., 1987: The development and verification of a cloud prediction scheme for the ECMWF model. *Quart. J. Roy. Meteor. Soc.,* **103,** 29–43.

Tanajura, C., 1996: *Modeling and Analysis of the South American Summer Climate.* Ph.D. dissertation, University of Maryland, 164 pp. [Available from University Microfilm, University of Maryland, College Park, MD 20742.]

Tiedtke, M., 1984: The effect of penetrative cumulus convection on the large-scale flow in a general circulation model. *Beitr. Phys. Atmos.,* **57,** 216–239.

Vernekar, A., B. Kirtman, J. Zhou, and D. Dewitt, 1992: Orographic gravity-wave drag effects on medium-range forecasts with a general circulation model. *Physical Processes in Atmospheric Models,* D. R. Sikka and S. S. Singh, Eds., Wiley Eastern Limited, 295–307.

Xie, P., and P. Arkin, 1996: Analysis of global monthly precipitation using gauge observations, satellite estimates, and numerical model predictions. *J. Climate,* **9,** 840–858.

Xue, Y., P. J. Sellers, J. L. Kinter, and J. Shukla, 1991: A simplified biosphere model for global climate studies. *J. Climate,* **4,** 345–364.

Zhao, Q., T. L. Black, and M. E. Baldwin, 1997: Implementation of the cloud prediction scheme in the Eta model at NCEP. *Wea. Forecasting,* **12,** 697–711.